Stanford Exploration Project, Report 111, June 9, 2002, pages 1–17

Subsalt event regularization with steering filters

Marie L. Prucha and Biondo L. Biondi[1]

ABSTRACT

The difficulties of imaging beneath salt bodies where illumination is poor are well known. In this paper, we present an angle-domain least-squares inversion scheme that regularizes the seismic image, tending to smooth along specified dips. This smoothing is accomplished using steering filters. We show the results of using the regularized inversion with smoothing along the angle axis and along both the angle and common midpoint axes. Additionally, the ramifications of specifying incorrect dips to smooth along will be examined. The results show that this regularized least-squares inversion does produce a cleaner, more continuous result under salt bodies. The inversion will reject incorrectly chosen dips used for the regularization.

INTRODUCTION

Obtaining a clean, coherent seismic image in areas of complex subsurface can be difficult. This is particularly true when the subsurface lends itself to shadow zones, such as those under the edges of salt bodies. In these areas, little of the seismic energy gets to the reflectors, and even less energy makes it back to the surface (Muerdter et al., 1996; Prucha et al., 1998). In addition to the shadow zones, proper imaging is made difficult by multipathing. Multipathing occurs when energy that follows different paths through the subsurface arrives at the receiver at the same time. Solving these issues is no simple matter.

It has been suggested that it is possible to eliminate artifacts caused by multipathing by imaging in the reflection angle domain via angle-domain Kirchhoff migration (Xu et al., 1998, 2001). However, Kirchhoff methods are not necessarily optimal for complex subsurfaces (SEG Workshop, 2001). Additionally, Stolk and Symes (2002) have shown that angle-domain Kirchhoff migration may not eliminate artifacts in strongly refracting media, even when using the correct velocity and all arrivals. To address these issues, angle-domain wave-equation migration methods have been developed (Prucha et al., 1999a,b; Fomel and Prucha, 1999; Sava et al., 2001). Stolk and De Hoop (2001) have shown that these methods do not suffer from image artifacts when migrated at the correct velocity.

Unfortunately, migration alone does not necessarily provide the best image. A better image in complex areas can often be obtained using least-squares inversion (Nemeth et al., 1999; Duquet and Marfurt, 1999; Ronen and Liner, 2000). However, inversion often cannot improve

[1]**email:** marie@sep.Stanford.EDU,biondo@sep.Stanford.EDU

the image in shadow zones without many iterations. With many iterations, noise in the null space caused by poor illumination can cause the inversion process to blow up.

To prevent these blow-ups, since we often have some idea of what the image in the shadow zone should look like, we can impose some sort of regularization on the inversion carried out in the angle domain (Prucha et al., 2000, 2001; Kuehl and Sacchi, 2001). In this paper, we will use a regularization that tends to create dips in the image from *a priori* selected reflectors and therefore can be applied by the use of steering filters (Clapp et al., 1997; Clapp, 2001). The inversion uses these steering filters to strengthen existing events to help fill in shadow zones. This regularization may even improve amplitude behavior (Prucha and Biondi, 2000).

The inversion process we use in this paper lends itself to two different regularization schemes. The "1-D approach" tends to create flat events along the reflection angle axis. This helps to fill in holes in different angle ranges caused by poor illumination. The "2-D approach" cascades the 1-D approach with an attempt to create dips along picked reflectors in the common midpoint (CMP) - depth plane. This allows the user to test possible interpretations within shadow zones. If the picked reflector doesn't cause the regularization to tend to create dips that interfere with the data, the model will contain those "new" dips. If the picked reflectors are incompatible with the data, the inversion will reject the dips.

In this paper, we will first review the theory and implementation of our inversion, then show the results of this regularized inversion scheme on a fairly complex synthetic model. We will then study the impact of the regularization operator more closely. Finally, we will discuss some of our future plans.

THEORY

Our inversion scheme is based on the angle-domain wave-equation migration explained by Prucha et al. (1999a). To summarize, this migration is carried out by downward continuing the wavefield in frequency space, slant stacking at each depth, and extracting the image at zero time. The result is an image in depth (z), common midpoint (CMP), and offset ray parameter (p_h) space. The offset ray parameter can be easily related to the reflection angle by:

$$\frac{\partial t}{\partial h} = p_h = \frac{2 \sin\theta \cos\phi}{V(z, cmp)}, \tag{1}$$

where θ is the reflection angle, ϕ is the geologic dip, and $V(z, cmp)$ is the velocity function in depth and CMP location.

The inversion procedure used in this paper can be expressed as fitting goals as follows:

$$\begin{aligned} \mathbf{d} &\approx \mathbf{L}\mathbf{m} \\ 0 &\approx \epsilon \mathbf{A}\mathbf{m}. \end{aligned} \tag{2}$$

The first equation is the "data fitting goal," meaning that it is responsible for making a model that is consistent with the data. The second equation is the "model styling goal," meaning that

it allows us to impose some idea of what the model should look like using the regularization operator **A**. The model styling goal also helps to prevent a divergent result.

In the data fitting goal, **d** is the input data and **m** is the image obtained through inversion. **L** is a linear operator, in this case it is the adjoint of the angle-domain wave-equation migration scheme summarized above and explained thoroughly by Prucha et al. (1999b). In the model styling goal, **A** is, as has already been mentioned, a regularization operator. ϵ controls the strength of the model styling.

Unfortunately, the inversion process described by Equation 2 can take many iterations to produce a satisfactory result. We can reduce the necessary number of iterations by making the problem a preconditioned one. We use the preconditioning transformation $\mathbf{m} = \mathbf{A^{-1}p}$ (Fomel et al., 1997; Fomel and Claerbout, 2002) to give us these fitting goals:

$$\begin{aligned} \mathbf{d} &\approx \mathbf{LA^{-1}p} \\ 0 &\approx \epsilon\mathbf{p}. \end{aligned} \tag{3}$$

$\mathbf{A^{-1}}$ is obtained by mapping the multi-dimensional regularization operator **A** to helical space and applying polynomial division (Claerbout, 1998).

The question now is what the preconditioning operator $\mathbf{A^{-1}}$ is. We have chosen to make this operator from steering filters (Clapp et al., 1997; Clapp, 2001) which tend to create dips along chosen reflectors. This paper includes results from two different preconditioning schemes. One is called the 1-D preconditioning scheme and simply acts horizontally along the offset ray parameter axis. The 2-D scheme acts along chosen dips on the CMP axis and horizontally along the offset ray parameter axis. To construct the preconditioning operator along the CMP axis, we pick "reflectors" that represent the dip we believe should be in a certain location, then interpolate the dips between the picked reflectors to cover the whole plane.

RESULTS

We applied our preconditioned inversion scheme to a synthetic dataset provided to us by SMAART JV. This dataset is designed to have a significant shadow zone underneath the salt body. The result of angle-domain wave-equation migration of this dataset can be seen in Figure 1. In the CMP-depth plane, note the severe decrease in amplitude of the reflectors as they go beneath the salt. In the offset ray parameter (p_h)-depth plane, there is a large decrease in amplitude at small p_h. It is most visible inside the oval drawn on the figure. We consider this to be a "hole" in the event, since there is energy at very small p_h and large p_h.

Figure 2 shows the result of 3 iterations of 1-D preconditioned inversion. Recall that the 1-D preconditioning scheme acts horizontally along the p_h axis. The most obvious result of this is a substantial increase in the signal to noise ratio. In the context of this paper, the more interesting result is the increase in strength of the events along the p_h axis. The "hole" that is circled in the p_h-depth plane is beginning to fill in. This in turn makes the reflectors in the CMP-depth plane appear to extend farther under the salt, with stronger amplitudes. This result

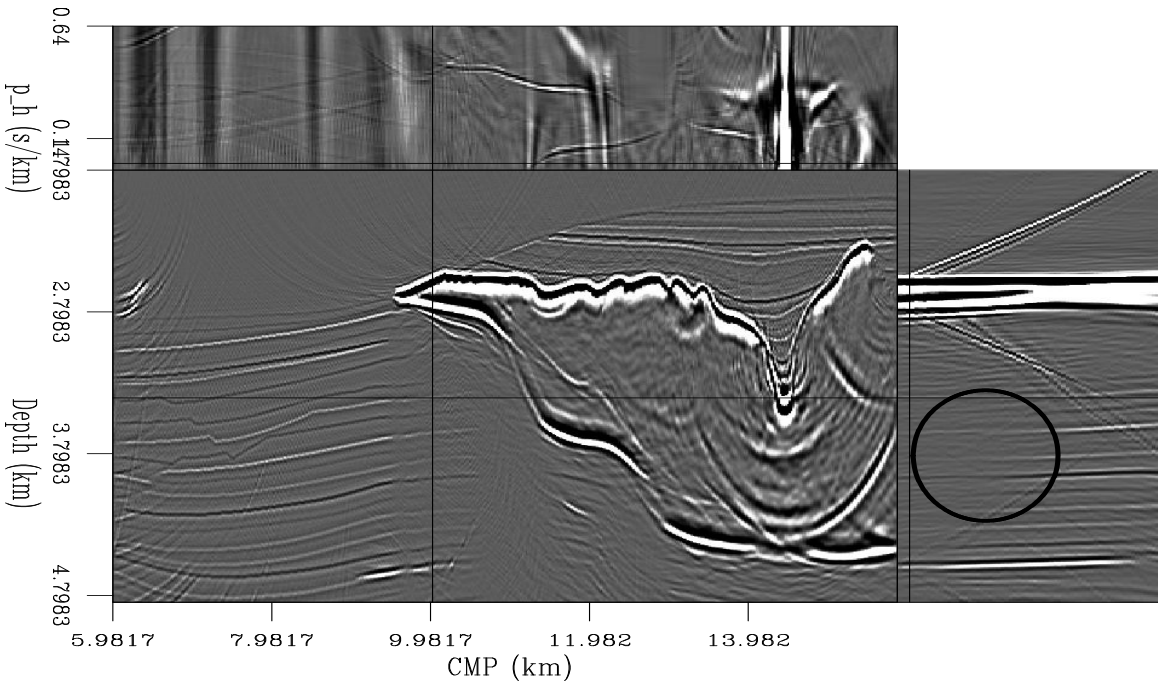

Figure 1: Result of angle-domain wave-equation migration. marie1-mig [CR]

is encouraging, but it seems likely that several more iterations would be necessary to really fill the hole.

To help fill in the shadow zones faster, we used our 2-D preconditioning scheme. To do this, we first picked reflectors in the CMP-depth plane (Fig. 3) to be used to create the preconditioning operator in this dimension. In the inversion, this operator was cascaded with the operator that smooths horizontally along the p_h axis.

The result of 3 iterations of the 2-D preconditioning scheme can be seen in Figure 4. This result is smooth and very promising. The hole in the p_h axis is gone and the reflectors extended underneath the salt with a stronger amplitude. Unfortunately, this method also creates some obvious errors in the output image. The top of the salt has lost some of its features because the picked reflector there was not detailed enough. Also, the faults at the left side of the image have been smoothed out. In this case, neither of these areas are of particular interest, but the problem of smoothing areas that shouldn't be smoothed is one we are trying to solve.

One way to reduce the smoothing effect is to follow several iterations of the preconditioned inversion (Equation 3), which tends to be smoother with fewer iterations, with a regularized inversion (Equation 2), which tends to be rougher with fewer iterations. The result of 3 iterations of preconditioned inversion followed by one iteration of regularized inversion can be seen in Figure 5. The result looks similar to the migration result (Fig. 1). Many events containing higher frequencies have been revived, including some of the processing artifacts. However, close examination of the areas of particular interest reveals important improvements.

In the CMP-depth plane, the reflectors going beneath the salt do not have the hole directly

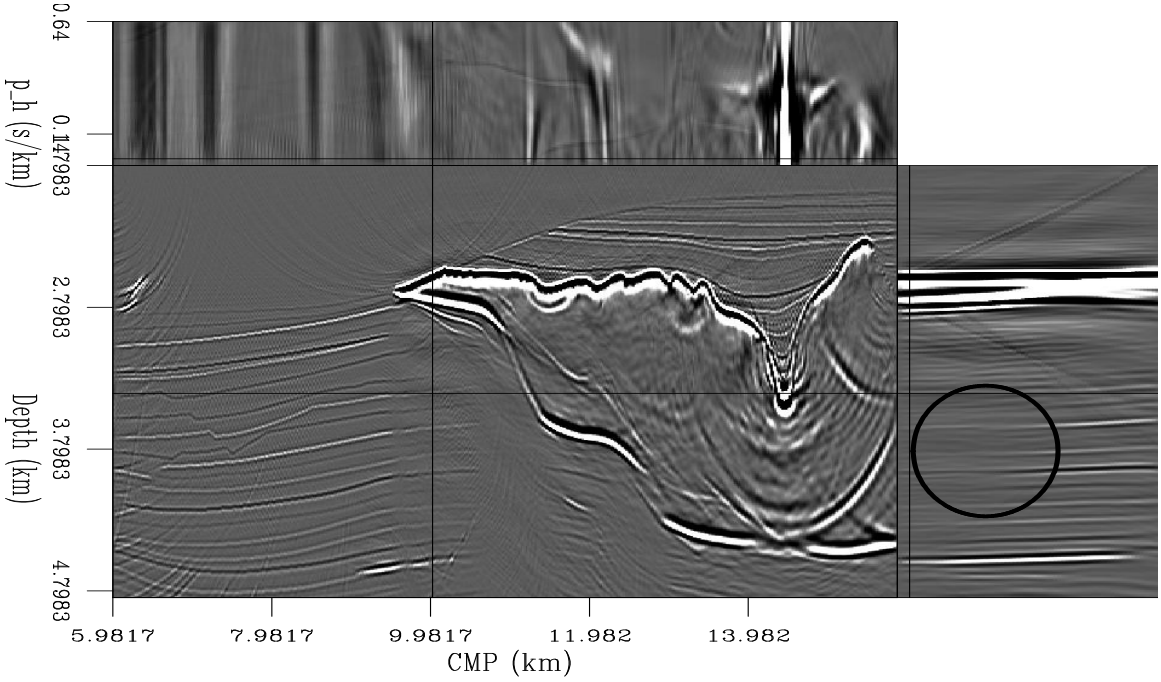

Figure 2: Result of 3 iterations of the 1-D preconditioned inversion. marie1-1dprec [CR]

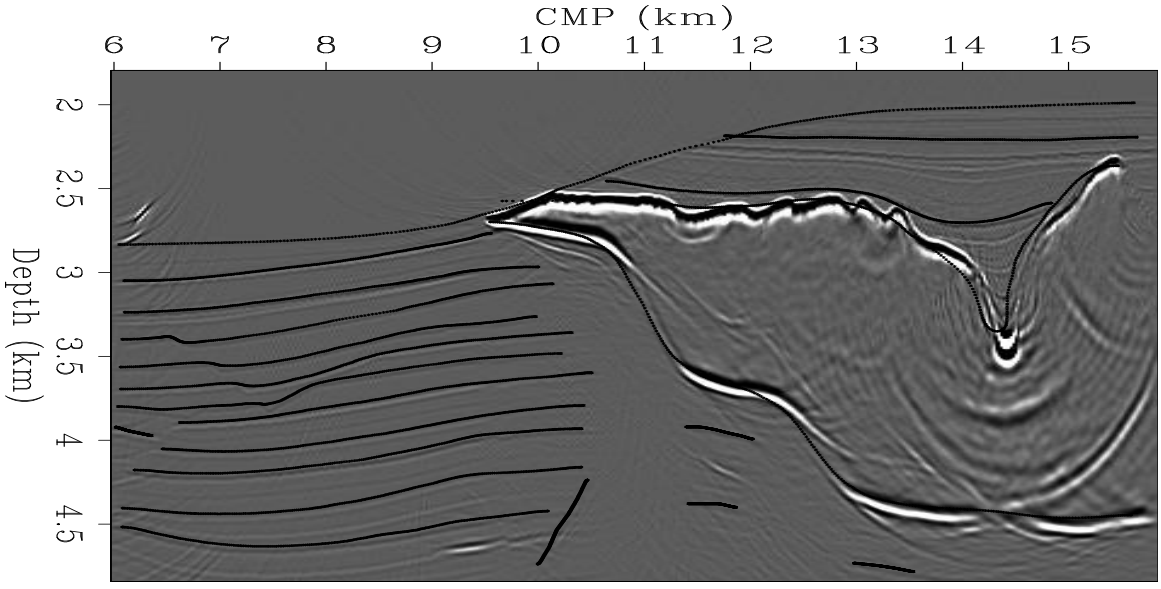

Figure 3: Migration result with picked reflectors for the 2-D preconditioned inversion overlaid. marie1-reflectors [CR]

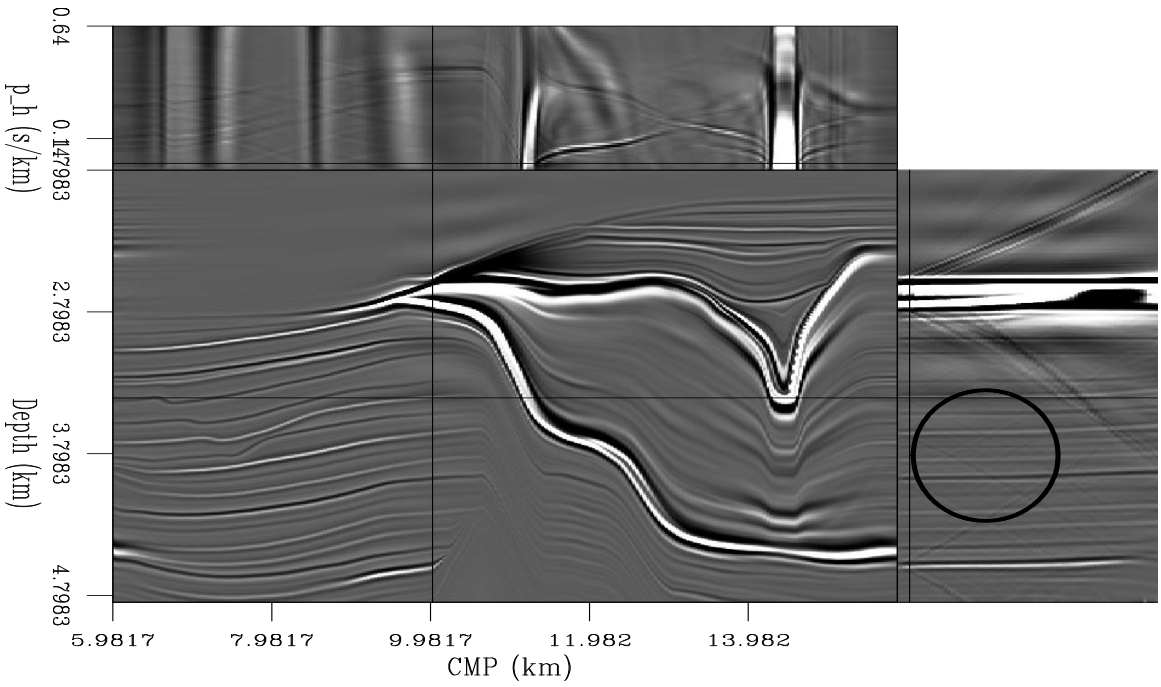

Figure 4: Result of 3 iterations of the 2-D preconditioned inversion. marie1-2dprec [CR]

beneath the tip of the salt that is seen in the migration result. In the circled area in the p_h-depth plane, the reflectors are more constant in amplitude than in the migrated result. These improvements could be increased with more iterations of regularized inversion. We are working on a way to determine a better combination of preconditioned and regularized iterations.

STEERING FILTER TEST

The previous results are promising, but it is clear that the 2-D inversion is strongly dependent on the preconditioning operator. Since this operator is constructed from picked reflectors, it is important to know what happens if the reflector is not picked well. To examine this, we created a preconditioning operator from the "reflectors" picked in Figure 6. In this figure, note that the picked reflectors cross the correct dips at the depths between 3 and 3.4 kilometers and 3.7 and 4.1 kilometers. They cross themselves at depth 4.5 kilometers. The picked reflector beginning at depth 3.75 km follows the correct dip for the most part, but ignores the slight change in dip at the fault at CMP position 7.2 km. The water bottom has been correctly picked. The picked reflector beginning at depth 4.2 km follows the correct dip, but continues well into the shadow zone where it may or may not be correct. Also within the shadow zone is a completely absurd picked reflector put there to see if any event can be created there. Finally, note that the top and bottom of the salt have not been picked at all. This will leave the preconditioning operator in the salt area to be interpolated from the picked reflectors. In this section, we will refer to the dips and reflectors from the migration result as "real" or "correct" and the dips and reflectors

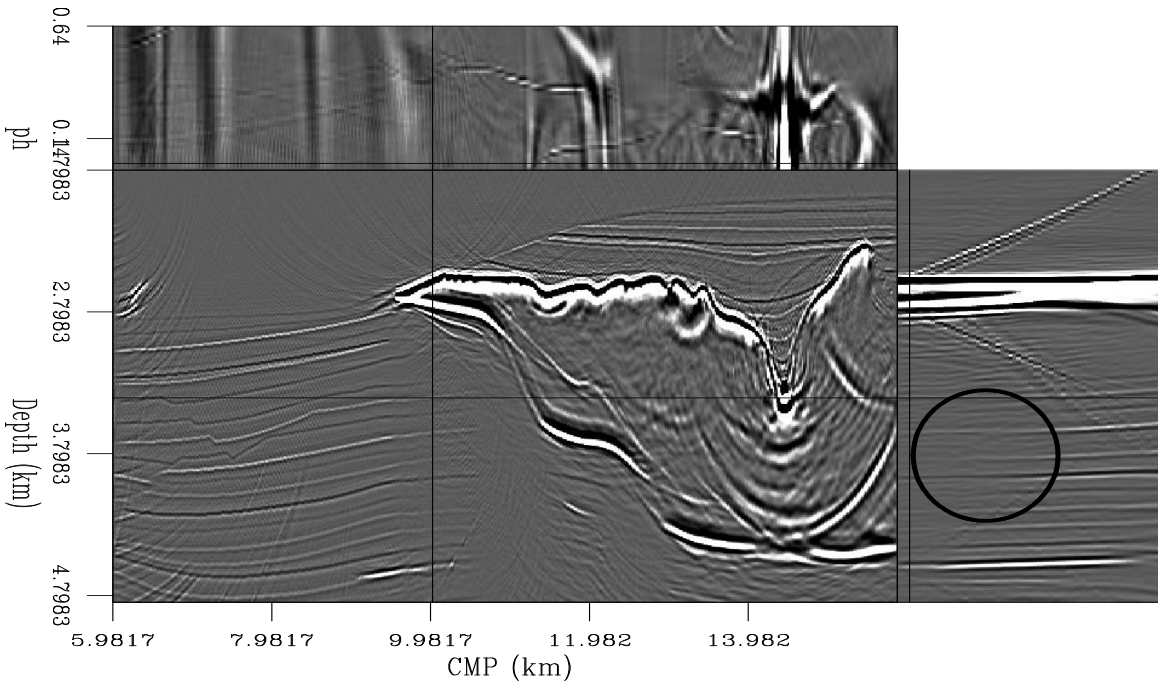

Figure 5: Result of 3 iterations of 2-D preconditioned inversion followed by 1 iteration of 2-D regularized inversion. marie1-2dprecreg [CR]

used for the inversion as "picked."

The result of using this preconditioning operator for the 2-D inversion is seen in Figure 7. As expected, the result isn't good. To investigate this closely, we chose 5 areas to look at as defined in Figure 8. In these areas, we calculated the instantaneous energy on both the migrated result and the result of the 2-D badly preconditioned inversion.

Box 1 enclosed an area in which the picked reflector began with an opposite dip to the correct one then changed to the correct one. In Figure 9, we can see that the energy from the migrated result is fairly constant all along the reflectors. In the panel from the inversion result, the energy has almost completely disappeared along the real reflectors where the picked reflector had the wrong dip, then recovers where the picked reflector has the correct dip. This example shows that picking dips that are completely wrong (opposite of the correct one) will cause the inversion to reject what the model styling goal (Eqn. 3) is trying to do.

In Box 2, the energy in the migrated panel is once again fairly constant along all of the reflectors (Fig. 10). In the preconditioned result, one of the most obvious effects is the loss of energy in the upper left corner. This loss of energy is caused by the picked reflector shown in Figure 9 which has the incorrect dip. The picked reflectors in Figure 10 are quite interesting. Both picked reflectors match the real events except where the real events are affected by faulting. For the shallower event, this results in energy loss at the beginning and end of the faulted area but little loss of energy elsewhere because the real dips are very close to the picked dips. For the deeper event, the faulted area has a different dip from the picked reflector, so the entire

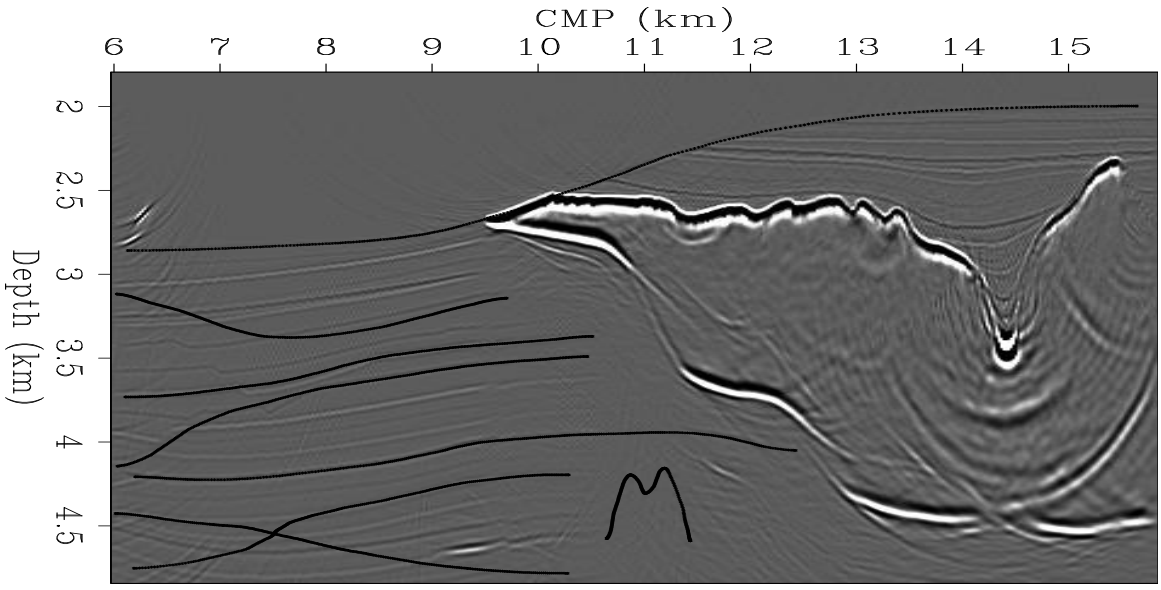

Figure 6: Migration result with the picked "reflectors" overlaid. These reflectors do not match the correct reflectors and should produce a bad result. marie1-reftest [CR]

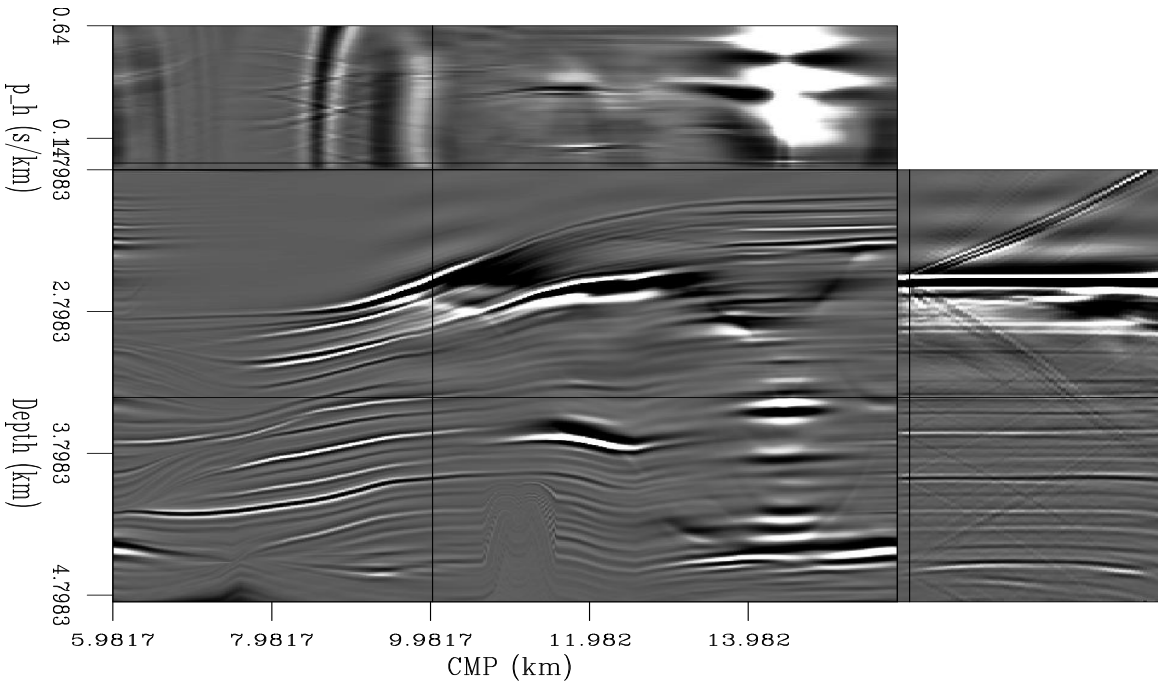

Figure 7: Result of 3 iterations of the 2-D preconditioned result with badly picked reflectors. marie1-2dfilttest [CR]

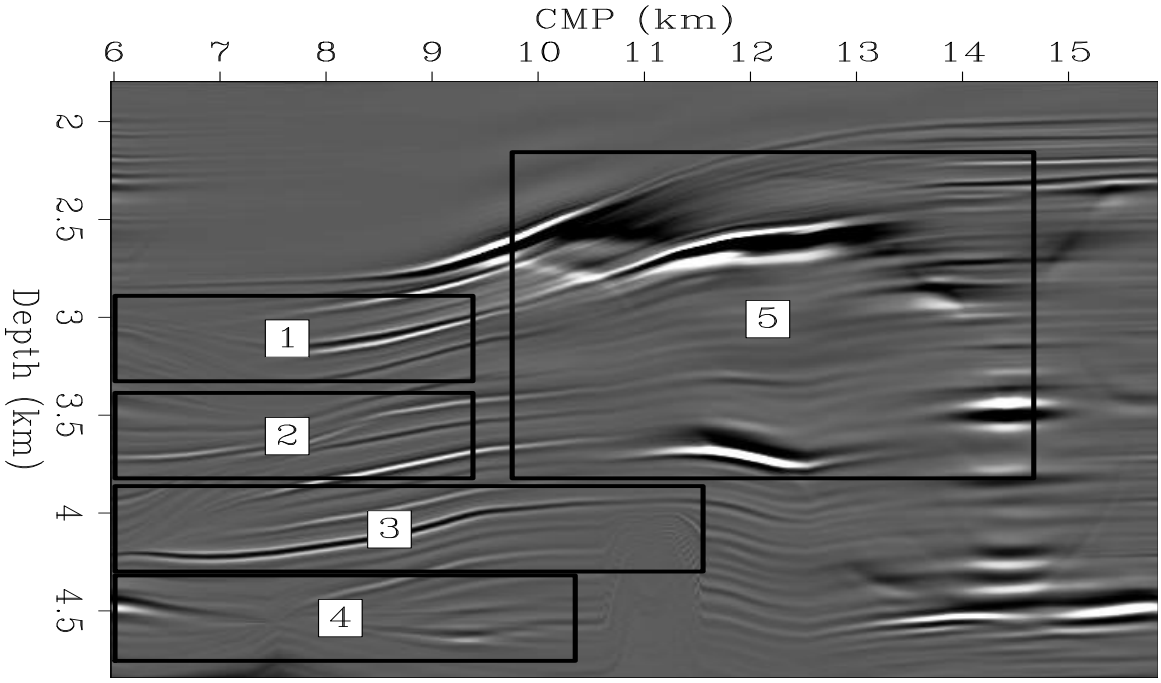

Figure 8: We will closely examine each of the boxed sections on this result of 3 iterations of the 2-D preconditioned inversion with badly picked reflectors. marie1-boxit [CR]

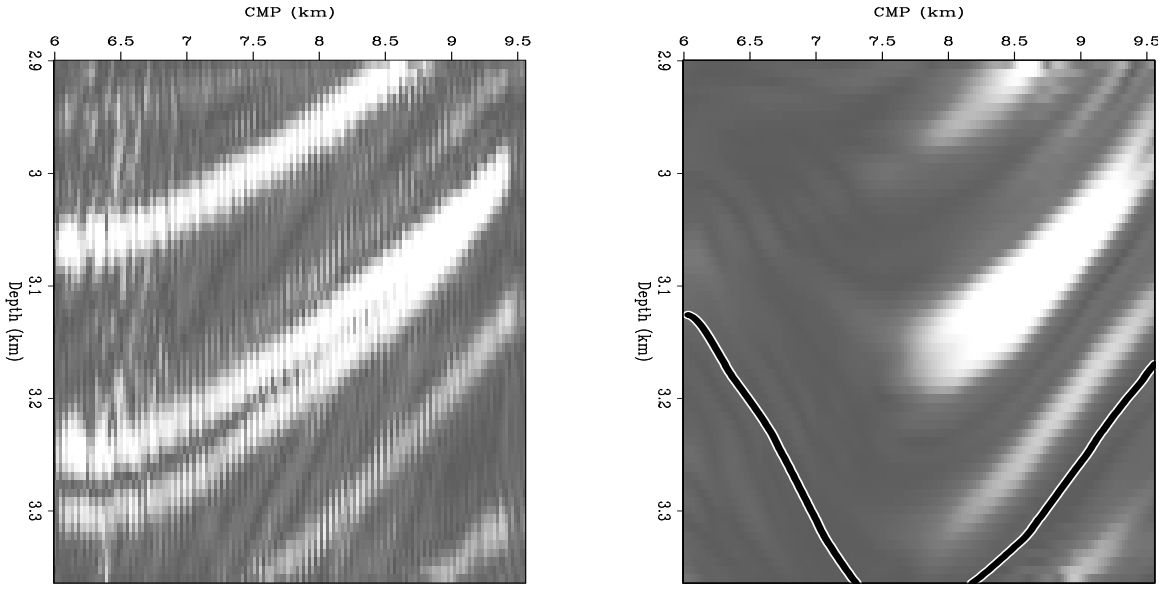

Figure 9: Energy comparison in Box 1. The left plot is from the migrated result, the right plot is from the 2-D preconditioned result with the picked reflector overlaid. The preconditioned result has very low energy where the picked reflector has the incorrect dip. marie1-comp.1 [CR,M]

faulted area has lost energy. This result may mean that this inversion scheme can be modified for fault detection. The deepest event in this box has lost no energy because it is close to the dip of the picked reflector above it. This example shows that the picked dip doesn't have to be totally different from the correct dip for the inversion to reject it.

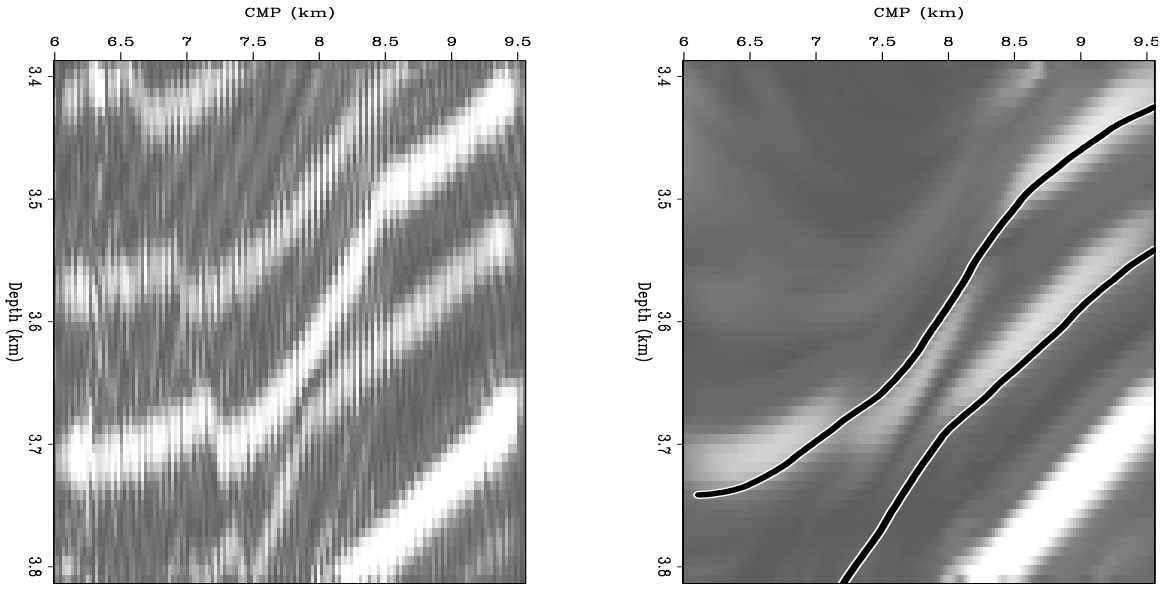

Figure 10: Energy comparison in Box 2. The left plot is from the migrated result, the right plot is from the 2-D preconditioned result with the picked reflectors overlaid. Once again, there is low energy where the dip of the picked reflector conflicts with the real dip. marie1-comp.2 [CR,M]

In Box 3, all of the coherent energy in the migrated result (Fig. 11) ends at CMP=9.5 km. The shallowest picked reflector in this box is the now-familiar incorrect dip reflector that causes the preconditioned result to lose energy in the upper left corner. The next two picked reflectors follow the real events but extend well beyond the coherent energy limit in the migrated result. This has caused the inversion to generate coherent energy well into the shadow zone beneath the salt. The final picked reflector in this box is the silly "M" shaped one that is entirely within the shadow zone. This picked reflector has had almost no effect on the energy of the preconditioned result, just as we would hope. This result clearly shows that the reasonably picked reflectors will enhance the result of the preconditioned inversion in shadow zones and that poorly picked reflectors in shadow zones won't generate unreasonable events.

The fourth area (Box 4) examined is very interesting. Here we wanted to test the stability of our inversion if the preconditioning operator contained conflicting dips. Figure 12 shows the energy from the migrated result is somewhat garbled along the left side and coherent with smoothly varying dips otherwise. There is also a bright spot that is in the real model at CMP=9.5 km. The picked reflectors only match the correct dips above the depth of 4.5 km. The energy from the preconditioned result is incoherent and weak except for a small section between the CMPs at 8 km and 9 km and above 4.5 km in depth. The garbled left side energy from the migrated result has been smeared into a large blob and the bright spot

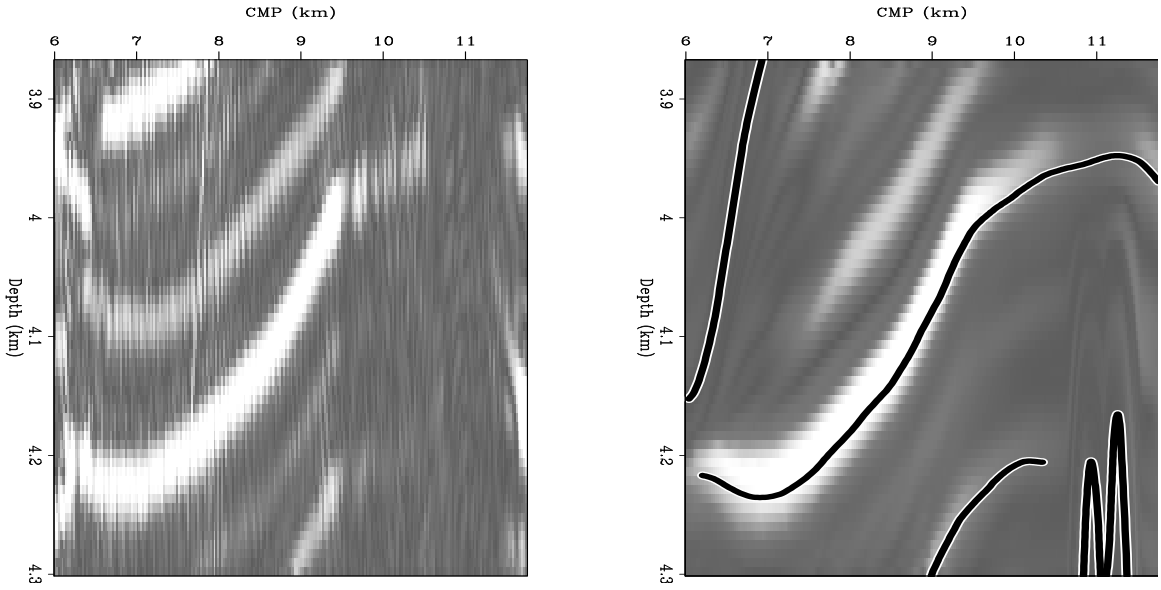

Figure 11: Energy comparison in Box 3. The left plot is from the migrated result, the right plot is from the 2-D preconditioned result with the picked reflectors overlaid. The reflectors were for the most part correctly picked for the preconditioned result, which does look better than the migrated result. marie1-comp.3 [CR,M]

has also been smudged. Overall this preconditioned result has managed to destroy almost all of the real information, just as expected. The important point from this experiment is that the preconditioned result did not show unexpected behavior in the area where the picked reflectors cross.

Box 5 contains part of the salt body. The only picked reflector really influencing this box was the water bottom. The energy from the migration shows high energy along the salt top and bottom, with low energy along the water bottom reflection and other layers (Fig. 13). The inversion has attempted to impose the dip of the water bottom on the salt events. The result has eliminated almost all of the energy that belonged to reflectors that were not close to the dip of the water bottom. This example shows that any strong reflectors that seem correct in the migration should be picked to preserve them in the inversion.

CONCLUSIONS

This paper has presented an inversion scheme that uses steering filters as a preconditioning operator. These steering filters tend to create dips along chosen reflectors. We presented a 1-D scheme in which the steering filters simply tried to act horizontally along the p_h axis and a 2-D scheme in which the tendency to create horizontal dips along the p_h axis was cascaded with steering filters tending to create dips along picked reflectors in the CMP-depth plane. Both of these methods increased the signal-to-noise ratio and helped to fill in the shadow zones.

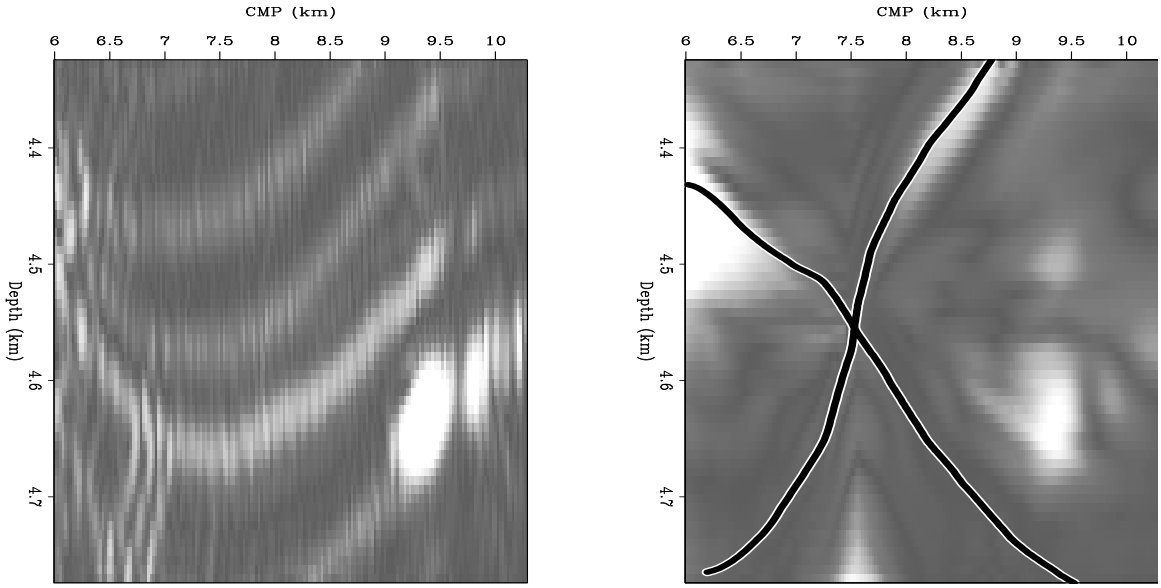

Figure 12: Energy comparison in Box 4. The left plot is from the migrated result, the right plot is from the 2-D preconditioned result with the picked reflectors overlaid. The preconditioned result because the picked reflectors had the incorrect dips almost everywhere. marie1-comp.4 [CR,M]

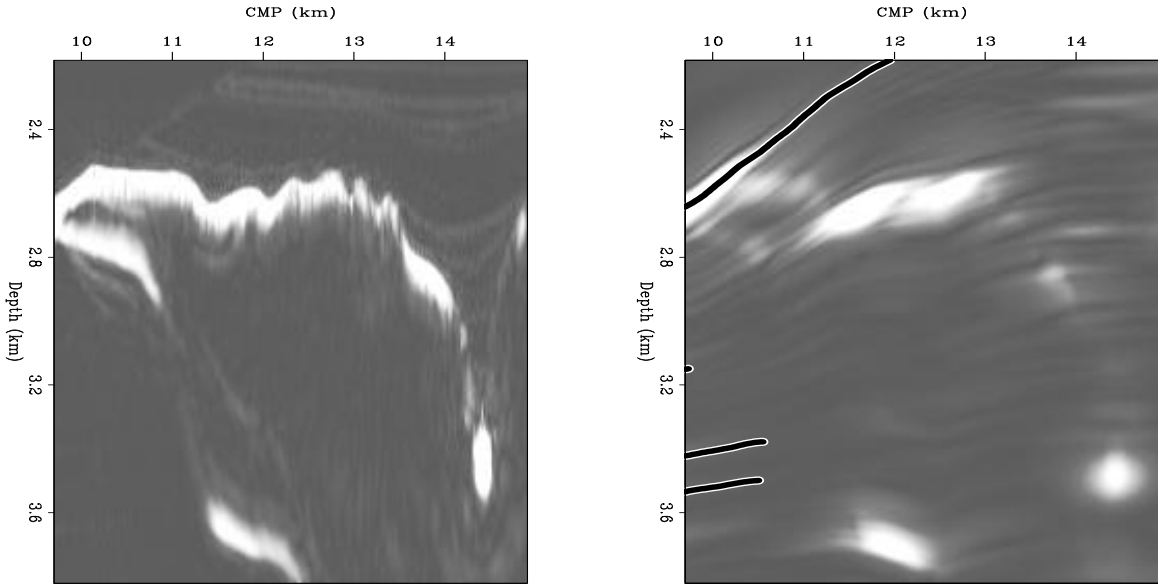

Figure 13: Energy comparison in Box 5. The left plot is from the migrated result, the right plot is from the 2-D preconditioned result with the very distant picked reflectors seen at the edges. The preconditioned result is horrible because the salt top and bottom were not picked. marie1-comp.5 [CR,M]

We also examined the effect of variation in the picked reflectors for the 2-D scheme. This was done by picking a variety of reflectors based on both the correct and the incorrect dips. This experiment showed that the inversion will reject dips that are incorrectly picked where data exists. This can even indicate areas where faulting has occurred. The inversion assures that picked dips that generate an event which interferes with the data are rejected. Picked dips that generate an event that doesn't interfere with existing data are allowed. Picked dips that cross, or meet at a point can be accommodated by the inversion. It is necessary to pick reflectors wherever the dominant dip changes.

FUTURE PLANS

We have several paths we would like to pursue soon. As mentioned above, we are trying to find a way to fine tune the combined preconditioning plus regularization scheme. Currently we are getting satisfactory results from carrying out more iterations of the preconditioned inversion than the regularized inversion, but we hope to find a way to determine the best combination. Additionally, it is not necessary to apply the preconditioning or regularization everywhere. Therefore we are working on a way to limit the effects of the preconditioning to a user-defined area. Another step that should be fairly straightforward is applying the entire process to 3-D data.

ACKNOWLEDGMENTS

We would like to thank SMAART JV for the synthetic dataset used in our experiments. Bob Clapp's advice on inversion, steering filters, and computer code has been invaluable.

REFERENCES

Claerbout, J., 1998, Multidimensional recursive filters via a helix: Geophysics, **63**, no. 5, 1532–1541.

Clapp, R. G., Fomel, S., and Claerbout, J., 1997, Solution steering with space-variant filters: SEP–**95**, 27–42.

Clapp, R. G., 2001, Geologically constrained migration velocity analysis: Ph.D. thesis, Stanford University.

Duquet, B., and Marfurt, K. J., 1999, Filtering coherent noise during prestack depth migration: Geophysics, **64**, no. 4, 1054–1066.

Fomel, S., and Claerbout, J., 2002, Multidimensional recursive filter preconditioning in geophysical estimati on problems: submitted to Geophysics.

Fomel, S., and Prucha, M., 1999, Angle-gather time migration: SEP–**100**, 141–150.

Fomel, S., Clapp, R., and Claerbout, J., 1997, Missing data interpolation by recursive filter preconditioning: SEP–**95**, 15–25.

Kuehl, H., and Sacchi, M., 2001, Generalized least-squares dsr migration using a common angle imaging condition: 71st Ann. Internat. Meeting, Soc. Expl. Geophysics, Expanded Abstracts, 1025–1028.

Muerdter, D. R., Lindsay, R. O., and Ratcliff, D. W., 1996, Imaging under the edges of salt sheets: a raytracing study: 66th Annual Internat. Mtg., Soc. Expl. Geophys., Expanded Abstracts, 578–580.

Nemeth, T., Wu, C., and Schuster, G. T., 1999, Least-squares migration of incomplete reflection data: Geophysics, **64**, no. 1, 208–221.

Prucha, M., and Biondi, B., 2000, Amplitudes and inversion in the reflection angle domain: SEP–**105**, 203–208.

Prucha, M. L., Clapp, R. G., and Biondi, B. L., 1998, Imaging under the edges of salt bodies: Analysis of an Elf North Sea dataset: SEP–**97**, 35–44.

Prucha, M., Biondi, B., and Symes, W., 1999a, Angle-domain common image gathers by wave-equation migration: 69th Ann. Internat. Meeting, Soc. Expl. Geophysics, Expanded Abstracts, 824–827.

Prucha, M. L., Biondi, B. L., and Symes, W. W., 1999b, Angle-domain common image gathers by wave-equation migration: SEP–**100**, 101–112.

Prucha, M. L., Clapp, R. G., and Biondi, B., 2000, Seismic image regularization in the reflection angle domain: SEP–**103**, 109–119.

Prucha, M. L., Clapp, R. G., and Biondi, B. L., 2001, Imaging under salt edges: A regularized least-squares inversion scheme: SEP–**108**, 91–104.

Ronen, S., and Liner, C. L., 2000, Least-squares DMO and migration: Geophysics, **65**, no. 5, 1364–1371.

Sava, P., Biondi, B., and Fomel, S., 2001, Amplitude-preserved common image gathers by wave-equation migration: 71st Ann. Internat. Meeting, Soc. Expl. Geophysics, Expanded Abstracts, 296–299.

SEG Workshop, 2001, Seismic imaging beyond Kirchhoff workshop: Society of Exploration Geophysicists.

Stolk, C., and De Hoop, M. V. Seismic inverse scattering in the 'wave-equation' approach:. Preprint 2001-047, The Mathematical Sciences Research I nstitute, 2001. http://msri.org/publications/preprints/2001.html.

Stolk, C., and Symes, W., 2002, Artifacts in Kirchhoff common image gathers: 72nd Annual Internat. Mtg., Soc. Expl. Geophys., Expanded Abstracts, submitted.

Xu, S., Chauris, H., Lambare, G., and Noble, M., 1998, Common angle image gather - A strategy for imaging complex media: 68th Annual Internat. Mtg., Society of Exploration Geophysicists, Expanded Abstracts, 1538–1541.

Xu, S., Chauris, H., Lambare, G., and Noble, M., 2001, Common angle image gather - A strategy for imaging complex media: Geophysics, **66**, no. 6, 1877–1894.


HOLLYWOOD TOWER
Hotel